MATERIALS CHEMISTRY FRONTIERS

CCS 中国化学会 CHINESE CHEMICAL SOCIETY

ICCAS

ROYAL SOCIETY OF CHEMISTRY

REVIEW

View Article Online
View Journal | View Issue

Cite this: *Mater. Chem. Front.*, 2023, **7**, 1896

Issues of phase segregation in wide-bandgap perovskites

Zhenhua Cui, Qingshan Zhang, Yang Bai * and Qi Chen *

Received 23rd December 2022,
Accepted 20th February 2023

DOI: 10.1039/d2qm01341j

rsc.li/frontiers-materials

Perovskite solar cells have attracted tremendous attention due to their rapid increase in efficiency and convenience of preparation. Among them, wide bandgap (WB) perovskites show advantages for tandem solar cell development and have become the most promising candidate for commercialization. However, stability issues crucially restrict the further development of WB perovskites. Due to their ionic nature, WB perovskites suffer severe photo-induced segregation and degradation under illumination. Therefore, in view of the above problems, we summarize the reasons for the instability of WB perovskites and discuss strategies for stability improvement. Finally, we provide prospects for the future development of WB perovskites.

1 Introduction

In the past decade, perovskite solar cells (PSCs), as a promising photovoltaic (PV) technology, have attracted tremendous attention due to their excellent power conversion efficiency (PCE) which has reached 25.7%[1] close to the theoretical limit of single-junction devices.[2] With a tunable band structure and a simple preparation process,[3,4] wide-bandgap (WB) perovskite materials (>1.65 eV) have been considered promising front cell candidates for tandem solar cell[5] development to exceed the theoretical limit.[6,7]

Perovskites have an ABX_3 structure, where A represents an organic (or inorganic) cation (such as Cs^+, FA^+, and MA^+), B is a divalent metal cation (typically Sn^{2+} and Pb^{2+}) and X is a halide anion.[8] The bandgap of perovskite materials can be tuned easily by controlling the cation ratio at the A site[9] and/or the halide ratio at the X site.[10] For MAPb $(I_yBr_{1-y})_3$ perovskites ($0 \leq y \leq 1$), their bandgap can be tuned from 1.58 eV to 2.38 eV as the ratio of iodide goes down.[11,12] However, problems such as local aggregation of halide ions and structural instability caused by ion migration may arise during film fabrication and device operation, which makes it difficult to maintain a high-quality and -stability photovoltaic device.[8] With the increase of bromide, perovskite films with segregated bromide-rich and iodide-rich phases were obtained instead of a homogeneous film.[3]

Beijing Key Laboratory of Construction Tailorable Advanced Functional Materials and Green Applications, MIIT Key Laboratory for Low-dimensional Quantum Structure and Devices, Experimental Center of Advanced Materials, School of Materials Science and Engineering, Beijing Institute of Technology, Advanced Research Institute of Multidisciplinary Science, Beijing 100081, P. R. China. E-mail: mse.ybai@bit.edu.cn, qic@bit.edu.cn

Zhenhua Cui

Zhenhua Cui received his BS degree in Materials Science and Engineering from the School of Materials Science and Engineering, Ocean University of China (OUC), in 2020. Currently, he is pursuing a master's degree under the supervision of Prof. Qi Chen and Prof. Yang Bai at the School of Materials Science & Technology, Beijing Institute of Technology (BIT). His current research interest focuses on the manipulation of perovskite film growth.

Yang Bai

Yang Bai received his BS degree (2013) from the School of Chemistry and Environment at Beihang University, and received his PhD degree (2017) from the Hong Kong University of Science and Technology (HKUST). He worked as a postdoc fellow at the Department of Chemistry, HKUST, under Prof. Shihe Yang's supervision. Now he is an associate professor at the Beijing Institute of Technology. His research focuses on perovskite solar cells and nanomaterials for optoelectronics.

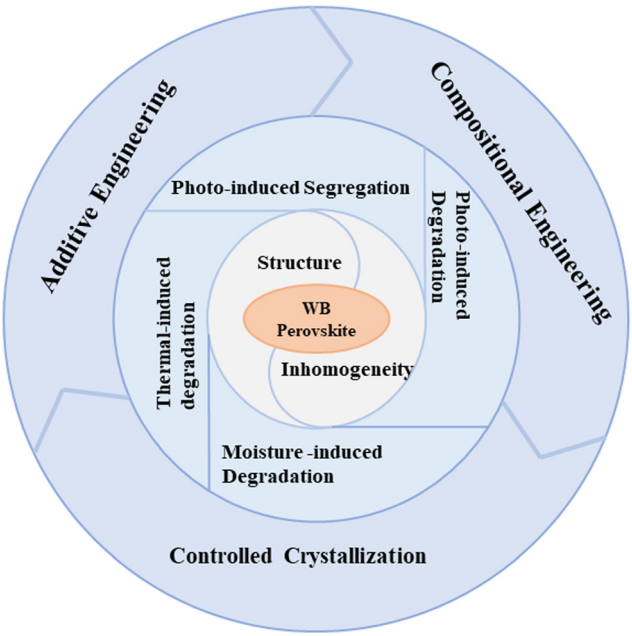

Fig. 1 Schematic illustration of the stability issues and strategies of WB perovskites.

In addition, phase segregation leads to the generation of a photoinduced trap, resulting in the loss of the open circuit voltage in the corresponding photovoltaic devices.[13]

In this review, we discuss the origin of phase segregation in WB perovskites, summarize the strategies for fabricating high quality films and inhibiting phase segregation, and propose the future development of WB perovskites (Fig. 1).

2 Properties of WB perovskites

The band gap of perovskites can be gradually tuned by replacing ions at the A, B, and/or X sites[14,15] (Fig. 2(a)). However, the change in ion ratios could also lead to variations in the Goldschmidt factor, which results in differences in the thermodynamical structure preference.[16]

Qi Chen

Qi Chen holds both his BS and MS degrees from Tsinghua University and received his PhD degree from the University of California, Los Angeles (UCLA). From 2013 to 2016, he worked as a postdoc fellow at California Nanosystem Institute (CNSI), UCLA, under Prof. Yang Yang's supervision. Now he is a professor at the Beijing Institute of Technology. His research focuses on hybrid materials design, processing and applications in optoelectronics and on energy harvesting and storage.

2.1 Structural properties of WB perovskites

Recently, mixed halide perovskites have been tremendously investigated for WB perovskite applications.[17] By tuning the y value (from 0 to 1) in $APb(I_{1-y}Br_y)_3$, the band gap of $FAPb(I_{1-y}Br_y)_3$ can be adjusted from 1.48 to 2.28 eV,[18] and 1.58 to 2.38 eV for $MAPb(I_{1-y}Br_y)_3$,[11] and 1.80 to 2.35 eV for $CsPb(I_{1-y}Br_y)_3$.[19] The band gap differences were initiated by a physical change in the Pb–X bond distance dictated by the ionic radius of halide anions.[20] Increasing the ratio of Br will lead to a decrease in the average bond distance of Pb–X,[19] resulting in lattice contraction and the increase of the corresponding band gap. Thus, in addition to band gap adjustment, the change in the anion ratio also affects the structural and electronic properties of perovskites.

The adjustment of the ion ratio in WB perovskites leads to structural distortion. For $MAPbX_3$, the pure triiodide composition has a distorted three-dimensional structure of the tetragonal *I*4/*mcm* space group, which differs from the cubic perovskite structure phase of the $Pm\bar{3}m$ space group in pure tribromide perovskite at room temperature (Fig. 2(b)).[21] The structure of perovskite begins to change as the ratio of bromide increases, in which the tetragonal phase is maintained until the ratio of Br reaches 0.13, and then it transits to a cubic phase when the ratio of Br reaches 0.2. The lattice spacing further decreases for the gradual substitution of larger I atoms with smaller Br atoms.[22] The Goldschmidt tolerance factor (t) is an empirical index for predicting the thermodynamically favorable structure of the perovskite material.[23,24] The Goldschmidt tolerance factor (t) can be calculated using the following expression:

$$t = \frac{R_A + R_X}{\sqrt{2}(R_B + R_X)}$$

where R_A, R_B, and R_X are the radius of the A site cation, B site cation, and X site anion, respectively. An orthorhombic, cubic, and hexagonal structure will form when $t < 0.8$, $0.8 < t < 1$, and $t > 1$, respectively.[20] By tuning the effective tolerance factor, Noh *et al.* demonstrated that the stable structure can be obtained by adjusting the ratio of I to Br.[22] Similarly, by adjusting the proportion of Cs^+ and FA^+ to achieve the regulation of tolerance factors, Li *et al.* improved the stability of the photoactive α-phase of $FA_{1-x}Cs_xPbI_3$.[16] The structure of the perovskite without Cs showed a large tolerance factor of 0.99, suggesting that it is stabilized in the hexagonal structure. In contrast, for the pure Cs perovskite, its small tolerance factor indicated that the orthorhombic phase was the most stable. With the increase of the Cs ratio, the formation-energy difference of the hexagonal and orthorhombic structure to cubic phase changes. When the ratio of Cs increased to 30%, the energy gap between δ-phases and α-phase reached a minimum value of 0.09 eV (Fig. 2(c)), indicating the enhanced stability of the α-phase. Although the FA/Cs perovskite slightly deviates from the WB perovskite, it provides a reference for the use of the factor.

Hence, adjusting the ratio of anions and cations can not only manipulate the band gap but also lead to structural distortion. The Goldschmidt tolerance factor (t) is a useful parameter to

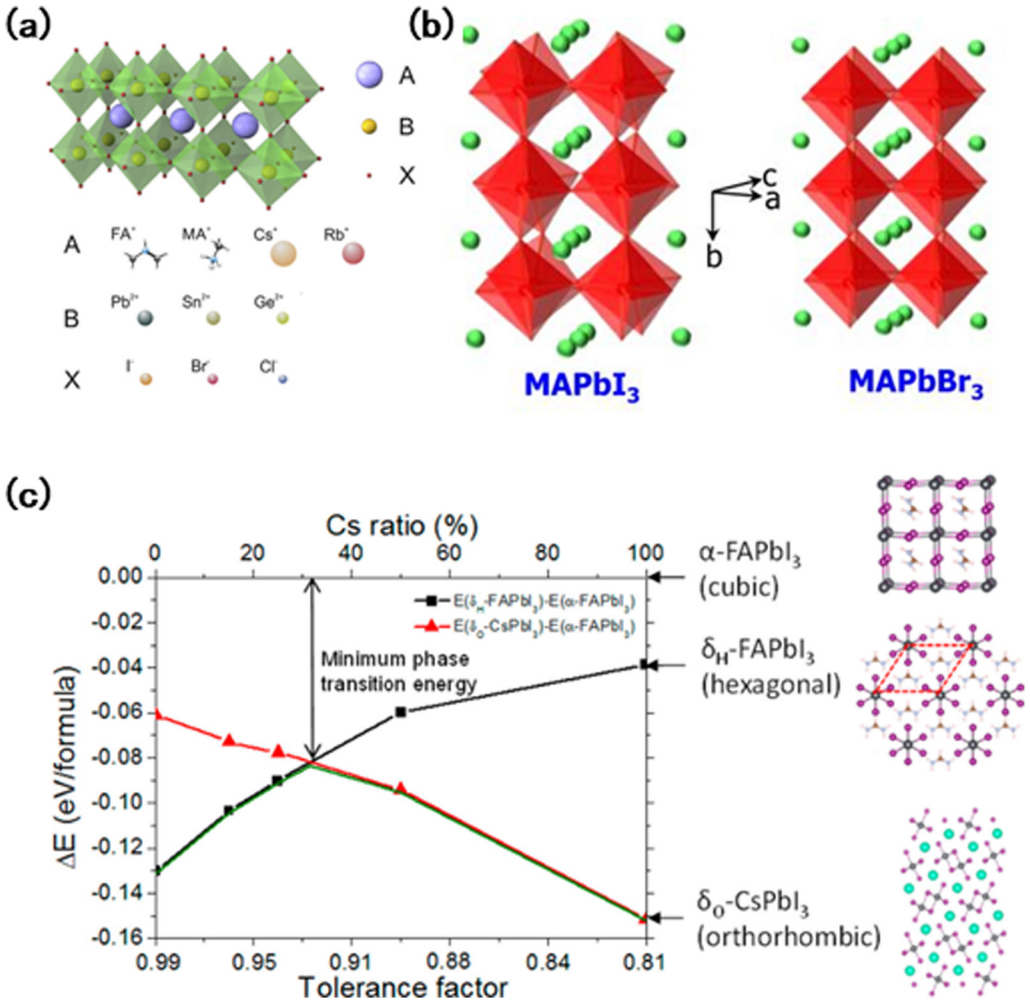

Fig. 2 (a) Schematic illustration of an ABX_3 perovskite and typical elements occupying the different positions in the structure.[8] (b) Distorted tetragonal perovskite structure of $MAPbI_3$ at room temperature and the cubic perovskite structure of $MAPbBr_3$ at room temperature. Red: polyhederon $(PbX_3)^-$; green: (MA^+).[22](c) Energy difference between the α-phase and different δ-phases of $FA_{1-x}Cs_xPbI_3$ alloys with different Cs ratios.[26]

predict structural changes and to guide the fabrication of stable perovskites.[16,25]

2.2 Film inhomogeneity in WB perovskites

In addition to the structural change, the film inhomogeneity of wide-bandgap perovskites is also a crucial issue for film production during composition modification, having a great impact on film stability.[27]

Adjusting the ratio of anions or cations is considered a simple method to modulate the band gap.[22] However, the compositional inhomogeneity has become a problem for the device performance.[28] Sadhanala *et al.* demonstrated that when the ratio of bromine (Br) increased to 20%, the presence of sub-bandgap states could be observed in the fresh $MAPb(I_{1-y}Br_y)_3$ $(0 \leq y \leq 1)$ films, which was interpreted as the initial formation of two phases (Fig. 3(a)).[3] The existence of a mixed phase will affect the carrier transfer with a decreased carrier lifetime. In $MAPb(I_{1-y}Br_y)_3$ films, as shown in Fig. 3(a), the photoluminescence (PL) peak position shifted from 2.23 to 1.57 eV during the change of the iodide ratio from 0 to 100%. However, when the iodide content increases to 0.4, shoulder peaks could be observed on the spectra, indicating the formation of a new photoactive phase and the coexistence of various phases. Besides, perovskites with this composition are prone to photoinduced phase segregation under light irradiation (Fig. 3(b)).[3]

Similarly, the problem of initial inhomogeneity and phase segregation also exists in WB perovskites with mixed cations.[29] In mixed cation perovskites, compared to inorganic cations, organic molecules usually alter the dielectric environment and shield electrons and holes due to their permanent molecular dipoles.[30] Besides, the addition of Cs^+ can assist the crystallization of the black phase of mixed $Cs_xFA_{(1-x)}PbI_3$ perovskites and fine-tune the Goldschmidt tolerance factor to enhance the structural stability.[31,32] However, phase segregation occurs in WB perovskite films when the Cs content is too high, due to the large size mismatch between Cs (1.81 Å) and FA (2.79 Å)/MA (2.70 Å),[33] putting the system in a high energy state and increasing the entropy preference for phase segregation. The introduction of inorganic cations can also result in the existence of incomplete hydrogen bonds (formed between organic cations,

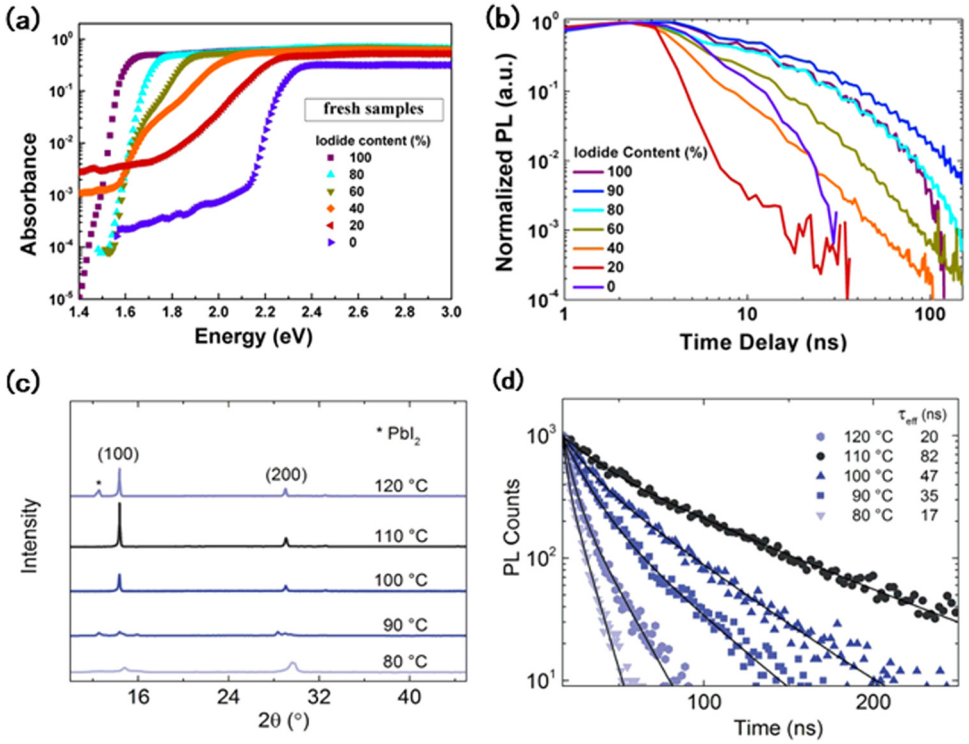

Fig. 3 (a) Photothermal deflection spectroscopy (PDS) measurements for 1 : 1 molar methylammonium lead–halide thin films with different iodide–bromide ratios.[3] (b) Plot of normalized PL intensity *versus* time for same films.[3] (c) XRD diffractograms of $MAPb(I_{0.6}Br_{0.4})_3$ films annealed at different temperatures for 90 mins.[38] (d) Time-resolution photoluminescence (TRPL) decay of $MAPb(I_{0.6}Br_{0.4})_3$ films annealed at different temperatures for 90 minutes.[38]

like MA^+ and FA^+, and halides), leaving active sites that can react or coordinate with water and other polar molecules. Uncoordinated reactive sites in non-uniform perovskite films[34] can cause nonradiative recombination of the carriers, reducing their lifetime and leading to the efficiency loss of the perovskite device.[3] Furthermore, in the $Cs_x(MA_{0.17}FA_{0.83})_{(1-x)}Pb\ (I_{0.83}Br_{0.17})_3$ system, deviation from the optimal Cs content ratio can result in a loss of up to 50 mV in V_{oc}, mainly due to the existence of recombination centers caused by the $CsPbI_3$ phases or 6H polytype of the perovskite in the film.[35] Moving away from the optimal WB perovskite ratio can also lead to an increase in impurities and a decrease in J_{sc} and FF.[16]

The film growth is not only determined by the composition, but also is influenced by fabrication conditions and solvents in the precursor solution.[36,37] Jaysankar *et al.* investigated the crystallization dynamics in a WB $MAPbI_{0.6}Br_{0.4}$ perovskite film.[38] They found that when the annealing temperature was below 100 °C or the annealing time was less than 30 mins, the precursor solution was unable to convert into a perovskite film completely, resulting in the existence of non-photoactive areas. However, extending the annealing temperature to 120 °C and the annealing time to 150 mins caused the film to degrade[39] (Fig. 3(c)). These regions could serve as sites for the non-radiative recombination of charge carriers, leading to a decrease in the charge carrier lifetime and the overall performance of the device. Moreover, inadequate annealing temperature and duration resulted in the reduced carrier lifetime and inferior film quality (Fig. 3(d)). For example, the open circuit voltage at an annealing temperature of 110 °C was 0.3 V higher than that at 90 °C under the same annealing duration, due to the production of large grains with a uniform size distribution, which improves the current collection capability.[38] In addition, the interaction between the composition and solvent species in the WB perovskite precursor solution also results in the generation of by-products.[22,40] In $MAPb(I_{1-y}Br_y)_3$ $(0 \leq y \leq 1)$, the rapid reaction between PbI_2 and MAI leads to the rapid formation of perovskites, shortening the time for the film to reach homogenization and preventing the formation of a highly uniform and dense surface.[41] The inhomogeneity of the film is a major problem that leads to efficiency decay and instability in WB perovskites and the corresponding devices. However, in addition to the issues that arise during the preparation process, the degradation of films under operation conditions is also a challenge for their future applications.[42]

3 Stability of WB perovskites under operation conditions

The stability of WB perovskites under operation conditions is the biggest challenge for their commercialization.[43,44] Although many groups are devoted to improving the PCE of WB perovskites, stability is still the biggest obstacle (Table 1). The instability of wide-bandgap perovskites can be mainly divided into two categories: light-induced short-term phase segregation

Table 1 Device performance and stability of wide bandgap perovskites

Materials	E_g (eV)	V_{oc} (V)	PCE (%)	Test conditions	Stability	Year
$Cs_{0.1}FA_{0.2}MA_{0.7}Pb(I_{1-x}Br_x)$	1.65	1.25	21.90	1 sun illumination; in air	550 h, 93%	2022[6]
$CsPbI_2Br$	1.91	1.27	16.25	RH < 20%; in air	60 d, 92%	2022[25]
$Cs_{0.2}FA_{0.8}Pb(I_{0.7}Br_{0.3})_3$	1.74	1.21	17.94	RT; in N_2	90 d, 87%	2021[37]
$Cs_{0.3}DMA_{0.2}MA_{0.5}PbI_3$	1.68	1.21	20.18	RT; maximum power point (MPP)	1000 h, 99%	2022[48]
CsFAMAPbIBr	1.63	1.13	20.35	RT; RH = 20%; in air	672 h, 86%	2021[53]
$FA_{0.8}Cs_{0.2}Pb(I_{0.7}Br_{0.3})_3$	1.70	1.19	18.30	AM 1.5G, 100 mW cm^{-2}; in N_2	400 h, 98%	2020[54]
$FA_{0.65}MA_{0.20}Cs_{0.15}Pb(I_{0.8}Br_{0.2})_3$	1.67	1.20	20.64	In the dark; RH = 50–60%; in air	25 d, 90%	2022[55]
$Cs_{0.15}FA_{0.85}Pb(I_{0.3}Br_{0.7})_3$	2.00	1.21	11.50			2017[56]
$FA_{0.65}MA_{0.20}Cs_{0.15}Pb(I_{0.8}Br_{0.2})$	1.68	1.17	19.80	Stable power output (SPO) measurement	4000 h, 96%	2019[57]
$FA_{0.65}MA_{0.20}Cs_{0.15}Pb(I_{0.8}Br_{0.2})$	1.75	1.18	16.80	MPP	14 d, 90%	2021[58]
$Cs_{0.2}FA_{0.8}PbI_{2.4}Br_{0.6}$	1.67	1.17	19.80	30 ± 5 °C; RH = 30 ± 5%; in the dark	1000 h, 81%	2022[59]
$Cs_{0.17}FA_{0.83}PbI_{3-x}Br_x$	1.70	1.08	16.40	In air	3500 h,80%	2021[60]
$Cs_{0.05}(FA_{0.77}MA_{0.23})_{0.95}Pb(I_{0.77}Br_{0.23})$	1.68	1.24	21.64	30 °C; MPP	70 h, 100%	2023[61]
$Cs_{0.2}FA_{0.8}PbI_2Br$	1.75	1.21	20.20	20–25 °C in the dark RH = 20–30%	1000 h, 100%	2022[62]

and long-term photothermal decomposition. However, light-induced phase segregation is the most common phenomenon of WB perovskites under illumination. The I-rich and Br-rich regions formed under operation conditions act as trap sites, reducing the charge mobility, shortening the carrier lifetime, and ultimately affecting the device performance.[45] In addition, WB perovskite materials are also prone to degradation under other external stimuli such as oxygen, humidity and heat.[46,47]

3.1 Photoinduced phase segregation

WB perovskites with an easily tunable bandgap are suitable for both single-junction solar cells and tandem solar cells.[48] However, compared with the band gap change caused by the tuning of the cation to anion ratio, V_{oc} promotion is quite limited.[49] Previous studies also demonstrated a decrease in V_{oc} during the increase of the band gap.[18,50] Hoke *et al.*[51] investigated the reason for V_{oc} decrease, which originated from photoinduced phase segregation. In $MAPb(I_{1-y}Br_y)_3$ ($0 \leq y \leq 1$) perovskites, an additional peak at 1.68 eV was observed in the photoluminescence (PL) spectra, indicating the existence of phase segregation (Fig. 4(a)). Moreover, after illumination, the XRD patterns of $(MA)Pb(Br_{0.6}I_{0.4})_3$ at 29.4° split into two peaks of 29.6° and 28.6°, which belonged to $(MA)Pb(Br_{0.7}I_{0.3})_3$ and $(MA)Pb(Br_{0.2}I_{0.8})_3$, respectively. Besides the polycrystalline film, phase segregation was also found in single crystals, implying that photoinduced phase segregation is an intrinsic property of WB perovskites.[51] Interestingly, photoinduced phase segregation is reversible and can be healed after several minutes in the dark. It can be observed in both mixed-anion and mixed-cation WB perovskites.[52]

As an ionic crystal, the photoinduced phase segregation of WB perovskites is the collective result of ion migration.[63] It is essential to understand the mechanism of phase segregation, the driving force of phase segregation, and the migration path and mechanism of segregation recovery. Ginsberg and co-workers proposed the polaron model of phase segregation to explain the original driving force of phase segregation.[64] Under illumination, free charges were formed as weakly bound electron–hole pairs which could rapidly dissociate, leading to the distortion of surrounding lattices through electron–phonon coupling. Then, excess free electrons interact with the distortion field to form dipoles leading to iodine-rich domains, and the size is limited by the deformation region of the polaron and cluster number by the total number of photogenerated charges (Fig. 4(c)). This model explained the initial dynamics of photoinduced phase segregation. Draguta *et al.* comprehensively explained the role of polarons in the whole process of photoinduced phase segregation.[65] According to the kinetic model shown in Fig. 4(b), the interaction between light and perovskites takes place in three paths: the first path is the light-excited perovskite material luminescence process, the second path shows the process of light-excited halogen anion rearrangement, and the last path indicates the interaction of photo-generated carriers with iodine-rich regions after diffusion. The last path is the process by which iodine clusters are created and gradually grow.

In addition to polycrystal films, photoinduced phase separation also exists in single nanocrystal (NC) WB perovskites.[66,67] The surface and grain boundary act as traps for photoinduced carriers, resulting in the presence of local electric fields in bulk perovskite films,[68] which also play an important role in the photoinduced phase segregation of WB perovskite single crystals. When photogenerated electron–hole pairs are present, the surface of a single crystal can capture one of them, leading to the formation of a local electric field on the surface, which becomes the initial site for phase segregation.[69] The electric fields generated by these carriers trapped on the crystal surface can further distort the lattice and generate local strain. Eventually, the iodide bonds break under the strain on the crystal lattice, leading to iodide migration. Interestingly, the reversal of phase segregation in the dark disappears in isolated single NCs, revealing that the existence of nearby NCs is essential for reversal to occur.[70]

Although studies have been conducted to investigate the formation mechanism of photoinduced phase segregation, little attention has been paid to the reversal process. In fact, the reversal of phase segregation is possible not only in the dark state, but also under light conditions.[70] Mao *et al.* achieved the regulation of phase segregation and reversal by adjusting the light intensity (Fig. 4(d)). In their proposed theoretical model, three forces determine the phase segregation and reversal process. Firstly, the generation of a strain field caused by the interaction between photogenerated carriers and halide ions acts as the driving force for the migration of iodide ions. Due to the bandgap funneling effect, the iodide ion clusters attract

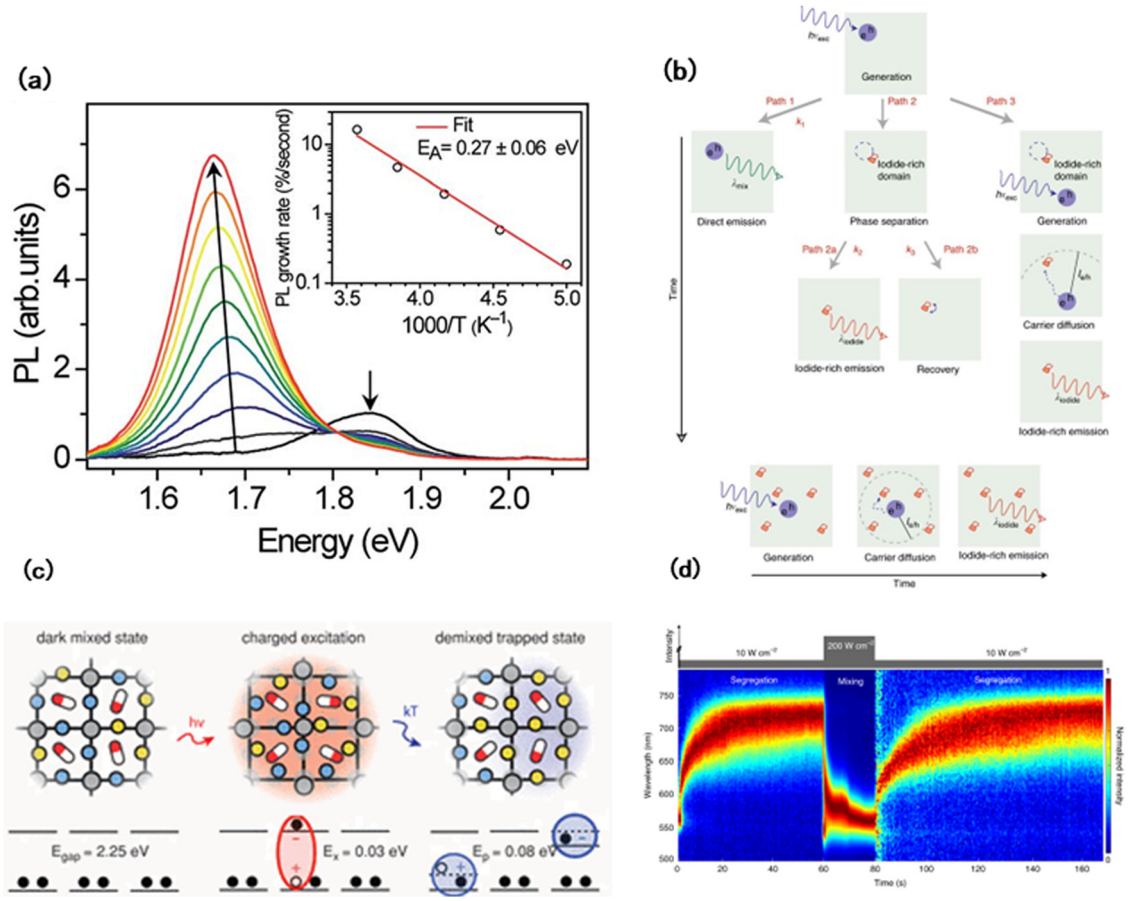

Fig. 4 (a) Splitting and shifting of PL spectra. Inset: Temperature dependence of the initial PL growth rate.[51] (b) Schematic of relevant kinetic processes during halide phase segregation.[65] (c) Photo-induced polaron trapping and associated energy scales associated with the phase.[64] (d) Photoinduced halide-ion segregation (PHS) and mixing (PHM) within a $MAPb(Br_{0.8}I_{0.2})_3$.[70]

carriers, resulting in cluster growth. Finally, under the action of high-intensity light, a large number of dipoles overlap, the driving force of the initial phase segregation disappears, and the concentration gradient starts to drive the phase segregation to recovery. Seog *et al.*[71] studied the phase segregation in halide-deficient and halide-rich perovskite films to illustrate the role of halides and their vacancies in the phase segregation and recovery process. When the halide is excessive, the speed of phase segregation is accelerated, but the final degree of phase segregation is relatively low. This is mainly due to the sufficient supply of halide ions leading to a reduction in the effective movement distance of the halide ions, but the interaction between Br and Pb hinders the further formation of phase segregation.

3.2 WB perovskite device performance under operation conditions

Much work has been done on the mechanism study of phase segregation, and its influence on WB perovskite device performance under operation conditions is also investigated. The presence of iodine-rich or bromine-rich regions due to photoinduced phase segregation dramatically affects the absorption and emission properties of WB perovskites.[65,72,73] Although the time of phase segregation is very short, the experimental results showed that the process was time dependent, and exhibits significant changes in absorption and emission behavior[22] Fig. 3(a) shows the variation of photoinduced phase segregation with time, and an emission peak appeared at ~550 nm (~2.25 eV) and slowly redshifts to ~710 nm (~1.75 eV) over the first 60 s under a pulsed laser with a low excitation intensity (10 W cm^{-2}), which greatly affected the light absorption of WB perovskites.[70]

As a result, photoinduced phase segregation leads to performance decay in the corresponding devices.[74] Samu *et al.* studied the impact of phase segregation on device performance. They demonstrated that the V_{oc} of the device decreased from 1.04 V to 0.91 V due to photoinduced phase segregation.[75] Besides, Li *et al.* observed a strong hysteresis with a hysteresis index of 47% in halogen hybrid perovskites, which was attributed to the work function change caused by ion accumulation between the perovskite layer and the transport layer.[76] Hu *et al.* further confirmed the effect of ion migration caused by photoinduced phase segregation at the interface.[77] The photovoltage changes with illumination, which originated from the redistribution of carriers at the interface caused by phase segregation, leading to energy band bending at the interface and the increase of the electron Fermi level, and finally an additional electrostatic

potential is generated. Recently, the impacts of phase segregation on device performance have been widely studied; however, there is still no consensus and the results are even controversial in some studies.[11,78]

Further prolonging the operation period, when the device was aged under continuous long-term illumination, irreversible photodegradation would take place. During this photodegradation process, an increase of the PbI_2 content was observed, which leads to device performance decay.[81] In the irreversible process, the perovskite decomposed into PbI_2, and at the same time, with the device configuration containing the TiO_2 electron transporting layer, deep trapping at oxygen vacancies on TiO_2 would strongly enhance the recombination, thus decreasing the performance of PSCs.[82] In addition, Norbert *et al.* proved that in the presence of light or ultraviolet light for a long time, $CH_3NH_3^+$ (MA^+) can be further decomposed into CH_3NH_2 and H_2 (Fig. 5(a)).[79] Several studies have demonstrated that photodegradation behavior is spectrum dependent, and ultraviolet (UV) radiation is the most damaging form of light.[83] Vlad *et al.* studied the relationship between the wavelength of light and film decomposition, they analyzed the *J–V* characteristics of PSCs at three different wavelengths of light, namely blue (470 nm), red (630 nm), and near infrared (NIR, 860 nm). They found that exposure to blue and red light sources leads to the formation of PbI_2, and the former case caused heavier damage.[81] And the light with an energy-rich dose is responsible for the formation of trap states, which accelerates the decomposition of the perovskite.[84]

3.3 Other factors affecting the stability of WB perovskites

During commercial and industry utilization, perovskite materials also suffered damage from other stimuli, such as moisture, oxygen, and thermalization, which could lead to irreversible material degradation.[80,85,86] Yang *et al.* studied the degradation mechanism of perovskites at high temperatures.[87] As the effect of light illumination, the photothermal phenomenon increases the temperature inside the perovskite films, resulting in a decrease in the light absorption rate and carrier transport capacity. Internal heat build-up leads to a decline in the EQE value (Fig. 5(b)) and performance decay in the corresponding device. The PCE, V_{oc}, and J_{sc} dropped by 44.2%, 22.3%, and 17%, respectively. In this process, WB perovskites will decompose layer by layer from the defect enrichment region, accompanied by lattice transition from the tetragonal phase to the PbI_2 trigonal phase (Fig. 5(c)).[80] Humidity and oxygen also greatly affect the stability of wide-gap perovskites,[88] especially in the presence of MA^+. Due to the instability of MA^+ itself, it would easily combine with water to form the monohydrate $CH_3NH_3PbI_3{\cdot}H_2O$ and the dihydrate $(CH_3NH_3)_4PbI_6{\cdot}2H_2O$, which accelerated the invasion of water and oxygen, leading to the fast degradation.[89]

From this point of view, the interaction between light and WB perovskites is complicated, and both photoinduced phase

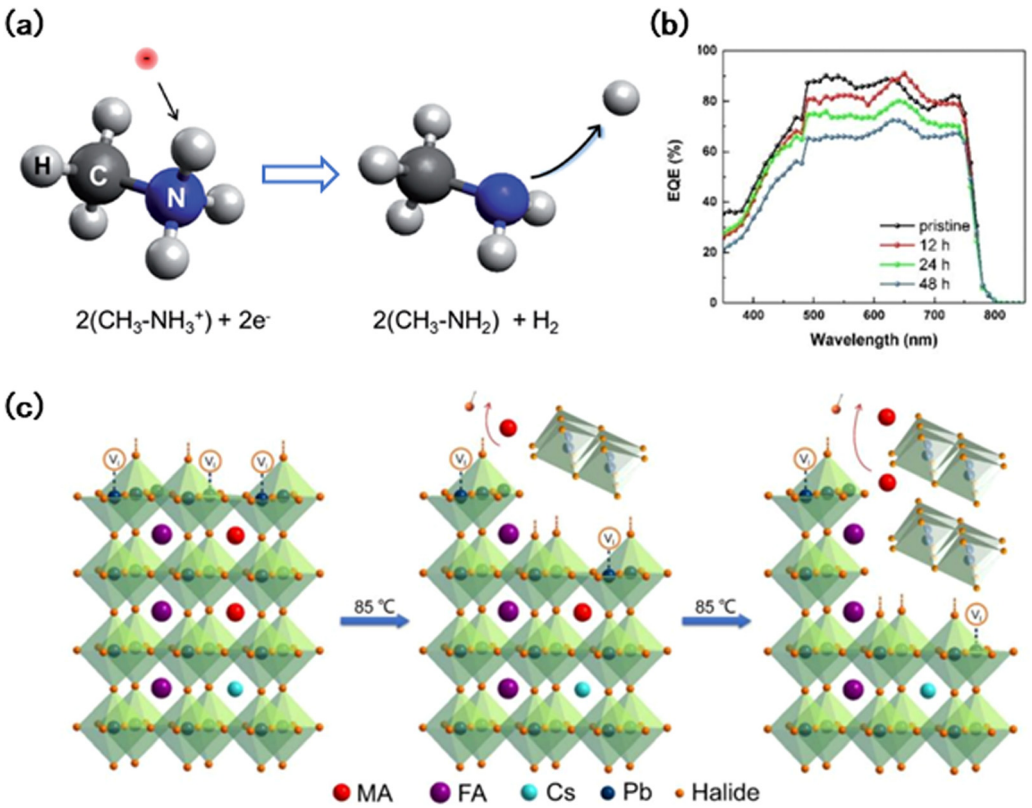

Fig. 5 (a) Schematic depiction of the dissociation mechanism of $CH_3NH_3^+$ due to the capture of a photogenerated electron.[79] (b) EQE spectra of the devices employing perovskite layers annealed for different durations.[80] (c) Schematic illustration of the proposed layer-by-layer degradation of the triple cation perovskite under 85 °C annealing.[80]

segregation and photodegradation existed. In addition, the presence of other stimuli like water, oxygen, heat, strain, *etc.*, can also accelerate film degradation through phase segregation, phase transition, and decomposition.[90–92]

4 Strategies for stability development in WB perovskites

4.1 Compositional engineering

The Goldschmidt tolerance factor of perovskites changes during the manipulation of perovskite composition. Therefore, adjusting the perovskite composition is also crucial for stability enhancement.

McMeekin *et al.* found it difficult to obtain continuous changes in the band gap of $FAPb(I_{1-y}Br_y)_3$ by simply manipulating the ratio of anions (Fig. 6(a)). During film preparation, structural instability caused the film to decompose dramatically, resulting in the presence of yellow phases in the as-prepared perovskite film.[52] In contrast, with the addition of Cs cations, the phase stability of the WB perovskites could be improved with expected bandgaps, improved crystal quality, and enhanced device performance. Compared to $MAPb(I_{0.6}Br0.4)_3$, the PL peak position of $FA_{0.83}Cs_{0.17}Pb(I_{0.6}Br_{0.4})_3$ was basically unchanged under irradiation after 60 min (Fig. 6(b)). The addition of Cs reduced the lattice constant, and a monotonic shift of the (100) reflection from 14.2° to 14.9° was observed, which revealed the lattice constant change from 6.306 to 5.955 Å. This indicated that the A-site cation can stabilize the perovskite with a photoactive α-phase by adjusting the lattice parameters. Several studies have proved that cationic compositional engineering has great advantages in regulating the structural stability, and the addition of a small amount of MA can also stabilize black-phase FA based perovskites with enhanced light absorption.[34] Saliba *et al.* found that the incorporation of Cs^+ would indeed improve the stability of $Cs_x(MA_{0.17}FA_{0.83})_{1-x}Pb(I_{0.83}Br_{0.17})_3$. However, the amount of Cs^+ needs to be well-controlled for performance improvement.

On this basis, alkali cations have attracted more and more attention. Fig. 6(c) shows the possible lattice sites that alkali cations can enter and occupy.[93] Recently, Rb^+ has been introduced as the A site cation to form quadruple-cation perovskites, which have achieved improved device performance.[94] The addition of Rb^+ increases the grain size of the perovskite film, which inhibited the invasion of oxygen along the grain boundaries, and film decomposition was significantly retarded. In addition to Rb^+, K^+ has also attracted attention. Limited by the smaller ion radius, they can hardly access the lattice sites but act as additives.[95] Given the excellent effect of inorganic cations in enhancing the stability of WB perovskites, the role of organic cations such as PEA^+, BA^+, GA^+ *etc.* has been widely investigated.[96] Compared with Cs^+, GA^+ has a larger ion size, which leads to lattice distortion. However, the FA–GA–Cs alloys can form a Fermi level close to the balance limit maximum, which resulted in enhanced phase stability in perovskite films.[97] In addition, the stable structure in the large-size cation system has significant compositional constraints, and the resultant phase is dependent on the mean tolerance factor and halide ratio, so it is difficult for pure large cations to form stable photoactive phases. Palmstrom *et al.* extended this suitability to a larger number of large-sized cations, such as acetamidinium, dimethylammonium (DMA), and methylenediammonium (MDA). The resultant device, which contained 10% DMA and 20% bromine, achieved a stable V_{oc} of 1.20 V, and an impressive long-term stability of 1000 h without obvious PCE decay (Fig. 6(d) and (e)).

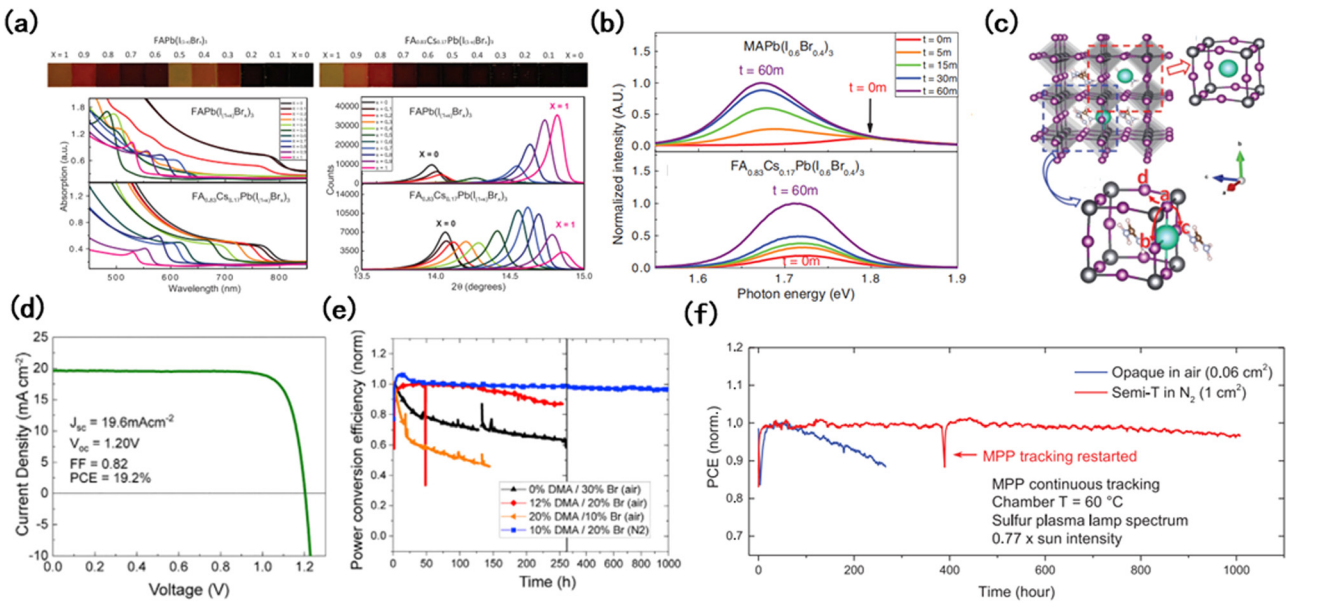

Fig. 6 (a) Comparison of performance changes caused by Cs incorporation.[52] (b) Normalized PL measurement measured after 0, 5, 15, 30, and 60 min of light exposure on the $MAPb(I_{0.6}Br_{0.4})_3$ and $FA_{0.83}Cs_{0.17}Pb(I_{0.6}Br_{0.4})_3$ thin films.[52] (c) Illustration of the possible locations of alkali cations in $FAPbI_3$: at the A site and the interstitial site.[93] (d) Current–voltage of the champion DMA-containing device.[98] (e) Long-term stability of perovskite devices with varying DMA and Br percentages.[98] (f) Long-term continuous MPP tracking under accelerated conditions.[99]

This strategy provides more options to tune the bandgap and avoid the addition of large amounts of bromine.[98]

Adjusting the anion at the X position has also been demonstrated to enhance the device stability without sacrificing performance. Xu *et al.* demonstrated the excellent performance of triple anion wide-bandgap perovskites (I/Br/Cl) in suppressing phase segregation and enhancing stability.[99] The introduced Cl entered the lattice successfully, further widening the band gap. And under the synergistic effect of Cs and Br, Cl was closer to the ideal size of the X site, benefiting the growth of uniform perovskite films with improved thermodynamic stability. After being tested in ambient air for 250 hours under MPP conditions, the device can still maintain 90% of the initial PCE (Fig. 6(f)). Junsang *et al.* investigated how Cl contributes to suppressing phase segregation. Due to the introduction of Cl, the migration of I/Br becomes more difficult, reducing the rate segregation constant between them by nearly four times. This is mainly due to the fact that Cl forms a more stable framework, increases the intensity threshold for segregation, increases the migration barrier of halide ions, and increases the ion migration activation energy of I/Br by about 4 kJ mol^{-1}.[100,101]

Changing the B site ions can also be used to adjust the structure of wide-bandgap perovskites and improve their stability. Various elements such as Ge, Eu, *etc.* have been used as B site additives, and have been shown to have a good effect on improving the phase stability.[76,102] However, the adjustment of B site ions is still challenging, and it was an obstacle due to ion oxidation and poor device performance.[103] Tuning the B site

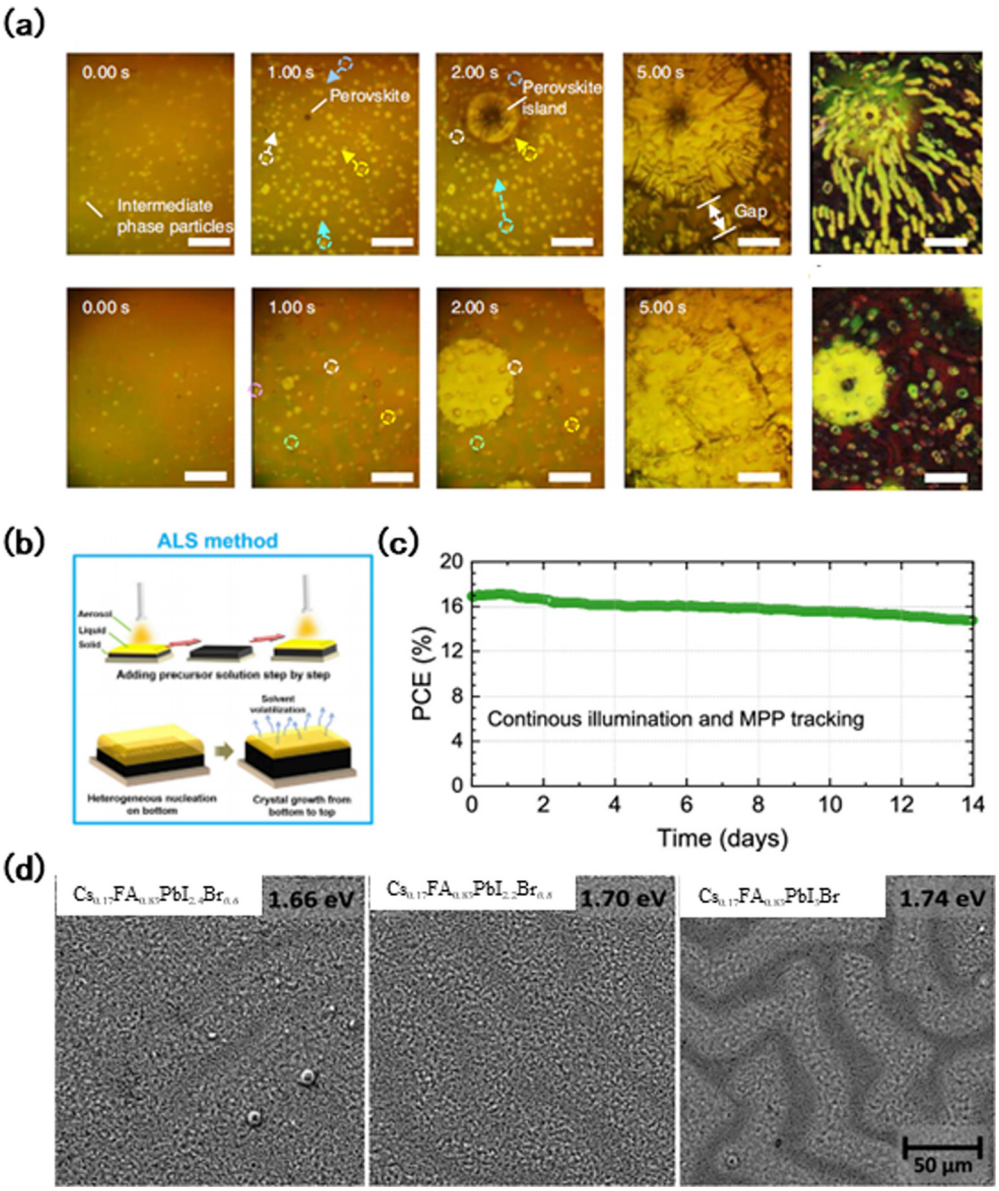

Fig. 7 (a) *In situ* microscopy observation of the ink layer drying dynamics.[105] (b) Schematic diagram of the ALS method.[106] (c) Stability assessment of wide-bandgap $FA_{0.65}Cs_{0.35}Pb(I_{0.73}Br_{0.27})_3$ perovskite solar cells with E_g = 1.75 eV, performed on encapsulated devices under a nitrogen atmosphere.[58] (d) Low magnification SEM images of the WBG perovskite layers on FTO-coated glass substrates, composed with different Br contents.[60]

ion is rarely used in current wide-bandgap perovskite development.

4.2 Controlled crystallization

Ion migration is an intrinsic feature in WB perovskites, which can be observed even in single crystals. The presence of defects can promote ion migration and accelerate the degradation of these perovskites.[104] Therefore, reducing the defect concentration in wide-bandgap perovskites will effectively improve the film and device stability, minimize non-radiative recombination, and enhance the device performance.[11] Improving the crystallinity of perovskite films to reduce the defect concentration has been widely investigated, especially for the production of large area films through blade-coating and spray-coating methods. Due to the problem of droplet contraction and difficulties of solution infiltration during the crystallization process, it is challenging to prepare large area high-quality perovskite films. Deng *et al.* added l-α-phosphatidylcholine (LP) surfactants to the solution, regulated the fluid flow dynamic process of the droplet and reduced the contraction effect of the island structure (Fig. 7(a)). As a result, a high-quality perovskite film was fabricated and achieved PCE values of 15.3% and 14.6% with active areas of 33 cm^2 and 57.2 cm^2, respectively.[105] Qian *et al.* obtained high-quality, low trap density perovskite films with an enlarged grain size by spray coating (Fig. 7(b)).[106] Benefiting from the aerosol–liquid–solid (ALS) assisted crystallization process, the perovskite embryo formed in the first stage grew continuously along the vertical direction and finally reached a steady state, resulting in the production of a uniform film. Lidón *et al.*[58] also noted the importance of obtaining homogeneous perovskite films and reported a method to prepare homogeneous WB perovskites. By using the alternative four-source vacuum deposition process, the relative ratio of Br/Cs can be uncoupled and controlled, resulting in a uniform distribution of Br and Cs. Based on this approach, they realized perovskites without phase segregation in the range of 1.7–1.8 eV and exhibited excellent stability. Under 300 mW cm^{-2} laser illumination, the PL intensity attenuation of this film is almost negligible after 1 hour, and through MPP tracking, 90% of the initial efficiency can still be maintained after 14 days (Fig. 7(c)).

In the wide band gap preparation process, the roughness of the perovskite film increases with the increase of the bromine content (Fig. 7(d)).[60] This is mainly attributed to the wrinkles formed on the surface due to compact stress during film formation.[107] Although the generation of wrinkles has been proved by Kevin *et al.*[108] to have little impact on the performance of the device, it may add obstacles to the subsequent processing steps of WB perovskites, such as the application of the charge transport layer and the passivation layer. They also proposed that the wrinkle morphology can be controlled by changing the anti-solvent and precursor solvent. The research of Ugur *et al.*[60] proved that the increase of the Br content will not only lead to the appearance of wrinkles, but also lead to the appearance of deep cracks and large-density non-radiative recombination centers, so they chose 1.7 eV perovskites for optimization. And finally, after 3500 hours of aging, 80% of the initial efficiency can still be maintained. The rapid crystallization caused by the increase of the bromine content will also lead to the formation of heterogeneous films. Jiang *et al.*[109] introduced a gas quenching method to induce top-down columnar growth of Br instead of its original disordered growth state. This method resulted in the lowest density of defects which effectively suppressed the segregation between I and Br, ultimately improving device stability. The obtained $Cs_{0.3}FA_{0.6}DMA_{0.1}Pb(I_{0.7}Br_{0.3})_3$ device can maintain 99% of the initial PCE for 2560 hours near the MPP.

As discussed before, annealing conditions, solution environments, material selection, and other factors also affect the quality of WB perovskites during film formation.[110,111] In detail controlling the crystallization of perovskite films towards high film quality and low defect density is important to further develop the device efficiency and long-term stability.

4.3 Additive engineering

In addition to manipulating the intrinsic materials to stabilize the structure and improve crystallization, additive engineering has also been widely adapted for performance and stability development. Zeng *et al.* showed that $Pb(Ac)_2$ can stabilize the α-phase perovskite.[110] The formation energy of the α-phase perovskite was reduced by the strong chemical interaction between carboxylic acid groups and Pb (Fig. 8(a)). After aging under 20 °C and 20% RH in air for 700 h, the perovskite device containing 5% $Pb(Ac)_2$ could still maintain more than 90% of the initial efficiency. At the same time, during the ripening process under high temperature conditions, a number of $Pb(Ac)_2$ decomposed into PbO and was located in the large grains, which helped in stabilizing the perovskite film.[112]

Defects such as vacancies and dangling bonds exist in large amounts in perovskite films and act as non-radioactive sites.[112] Jalebi *et al.* showed that K^+, as a passivator, could occupy the vacancies and coordinate with the dangling bonds at grain boundaries and interfaces. It led to a significant reduction in the rate of carrier recombination, improving the optoelectronic properties of perovskites, and also having an excellent effect on developing the interface between electrodes (Fig. 8(b)).[95] K^+ exhibits excellent performance in eliminating dangling bonds, vacancies, and other defects. To further explore the application of alkali cations, Cao *et al.* introduced various alkali cations such as Rb^+, Na^+, and Li^+ for the fabrication of perovskites. They found that the alkali cations could occupy the interstitial sites in perovskite lattices and raise the migration energy barrier for native halide defects, leading to improved photostability (Fig. 8(c)).[93]

Pseudohalogen additives have shown excellent performance in controlling perovskite crystal growth and defect passivation.[113] $Pb(SCN)_2$ and $PEA(I_{0.25}SCN_{0.75})$ have been applied to reduce defects by promoting the crystallization of perovskites and suppressing the generation of non-perovskite phases.[114] Benefiting from the $Pb(SCN)_2$ assisted crystallization and FAX passivation on the grain boundary, Zhou *et al.* obtained high-quality wide-bandgap perovskite thin films. The corresponding device showed an impressive efficiency of 18.6% with enhanced stability, which

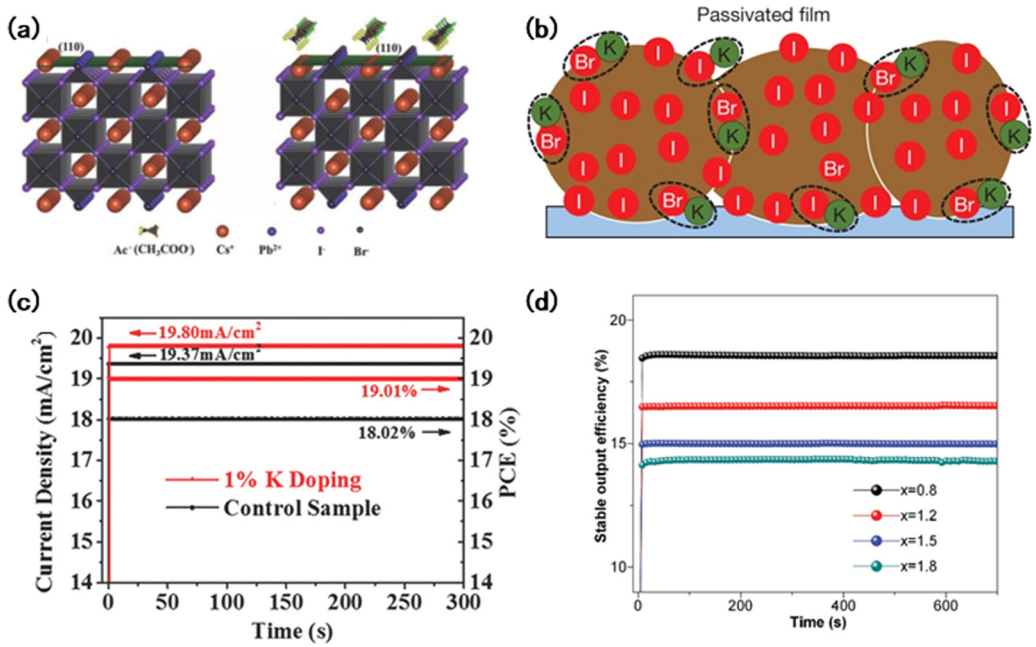

Fig. 8 (a) Schema of the $CsPbI_2Br$ (110) surface without and with Ac^- interaction.[110] (b) Schematic of the surplus halide is immobilized by complexing with potassium into benign compounds at the grain boundaries and surfaces.[95] (c) Steady-state current density and PCE of the PSCs without doping and with 1% K^+ doping.[93] (d) Stable output efficiency of the champion cells of $FA_{0.17}Cs_{0.83}PbI_{3-x}Br_x$ (x = 0.8, 1.2, 1.5, and 1.8) stressed at 1.06, 1.08, 1.08, and 1.10 V under 1 sun illumination, respectively.[115]

presented no PCE loss after 700 h under 1 sun illumination aging (Fig. 8(d)).[115] Kim *et al.* also proved that SCN could benefit the growth of films with a larger grain size, enhanced surface flatness, prolonged carrier lifetime, *etc.*[113] Compared to PEAI, PEA($I_{0.25}$-$SCN_{0.75}$) demonstrated a better effect with an increase in the grain size, and the stability of the corresponding device was greatly improved, which maintained about 80% of the initial efficiency after 1000 h under light treatment.

5 Conclusion and perspective

In summary, the structure of perovskites determines their optoelectronic properties, and their stability from a thermodynamic perspective. In particular, with complicated compositions, controlling the phase structure becomes the first priority for stabilizing WB perovskites. As the main reason for the instability of WB perovskites, avoiding the generation of non-perovskite phases and co-existence of various phases is crucial to inhibit the formation of heterogeneous structures during film fabrication, to suppress the ion migration and aggregation under light and thermal treatment, to protect the film from the invasion of water and oxygen molecules, *etc.* To improve the film quality and to impede ion migration, various kinds of strategies, including compositional engineering, crystallization manipulation and additive engineering, have been proposed, and demonstrated a dramatic improvement in the device efficiency and long-term stability.

Recently, the photoinduced phase segregation phenomenon in WB perovskites has been widely studied and the theory is relatively established. However, the mechanism study is far from satisfactory. Besides phase segregation, light illumination could also lead to film decomposition, and the mechanism is still unclear and needs to be investigated. In addition, the origin of film decomposition, the impact of the initial decomposition products on the structural stability of WB perovskites, and its influence on the subsequent degradation remain unclear.

For commercialization, several efforts still need to be made in WB perovskites. Firstly, the development of large-scale production of WB perovskites, as promising candidates for tandem devices, is urgent. Although methods such as slot-die coating, doctor blade coating, and spray coating have been introduced for perovskite film fabrication, their application in WB perovskite production is less studied, and the control of film homogeneity remains a challenge for these methods. Secondly, ion migration induced material degradation or decomposition should be inhibited. Mixed cation and low-dimensional WB perovskites may provide a solution to prevent fast halide migration, however, the issues of second phases and lower carrier mobility are also important. Thirdly, the influence of film inhomogeneity on the photoelectrical properties at various scales, from the atomic scale to the nanoscale and macro scale, needs to be clarified, which is necessary to fast locate the problem when facing material or device degradation. Finally, just like investigations in perovskites with a conventional band gap, the thermodynamic and kinetic control of crystallization, the composition of the precursor solution, conditions of the fabrication process, construction of interfaces, and selection of transport layer materials are equally important in the study of WB perovskite materials.

Conflicts of interest

There are no conflicts to declare.

Acknowledgements

The authors acknowledge funding support from the National Natural Science Foundation of China (52172182, U21A20172, 21975028, 22011540377) and the Beijing Municipal Natural Science Foundation (JQ19008).

References

1 H. Min, D. Y. Lee, J. Kim, G. Kim, K. S. Lee, J. Kim, M. J. Paik, Y. K. Kim, K. S. Kim and M. G. Kim, Perovskite solar cells with atomically coherent interlayers on SnO_2 electrodes, *Nature*, 2021, **598**(7881), 444–450.

2 W. Shockley and H. J. Queisser, Detailed balance limit of efficiency of p–n junction solar cells, *J. Appl. Phys.*, 1961, **32**(3), 510–519.

3 A. Sadhanala, F. Deschler, T. H. Thomas, S. E. Dutton, K. C. Goedel, F. C. Hanusch, M. L. Lai, U. Steiner, T. Bein and P. Docampo, Preparation of single-phase films of $CH_3NH_3Pb(I_{1-x}Br_x)_3$ with sharp optical band edges, *J. Phys. Chem. Lett.*, 2014, **5**(15), 2501–2505.

4 K. Choi, M. J. Jeong, S. Lee, G. Alosaimi, J. Seidel, J. S. Yun and J. H. Noh, Suppressing Halide Segregation in Wide-Band-Gap Mixed-Halide Perovskite Layers through Post-Hot Pressing, *ACS Appl. Mater. Interfaces*, 2022, **14**(21), 24341–24350.

5 C. Yan, J. Huang, D. Li and G. Li, Recent progress of metal-halide perovskite-based tandem solar cells, *Mater. Chem. Front.*, 2021, **5**(12), 4538–4564.

6 G. Yang, Z. Ni, Z. J. Yu, B. W. Larson, Z. Yu, B. Chen, A. Alasfour, X. Xiao, J. M. Luther and Z. C. Holman, Defect engineering in wide-bandgap perovskites for efficient perovskite–silicon tandem solar cells, *Nat. Photonics*, 2022, **16**(8), 588–594.

7 A. De Vos, Detailed balance limit of the efficiency of tandem solar cells, *J. Phys. D: Appl. Phys.*, 1980, **13**(5), 839.

8 M. Anaya, G. Lozano, M. E. Calvo and H. Míguez, ABX_3 Perovskites for Tandem Solar Cells, *Joule*, 2017, **1**(4), 769–793.

9 M. Saliba, T. Matsui, K. Domanski, J.-Y. Seo, A. Ummadisingu, S. M. Zakeeruddin, J.-P. Correa-Baena, W. R. Tress, A. Abate and A. Hagfeldt, Incorporation of rubidium cations into perovskite solar cells improves photovoltaic performance, *Science*, 2016, **354**(6309), 206–209.

10 C. M. Sutter-Fella, Y. Li, M. Amani, J. W. Ager III, F. M. Toma, E. Yablonovitch, I. D. Sharp and A. Javey, High photoluminescence quantum yield in band gap tunable bromide containing mixed halide perovskites, *Nano Lett.*, 2016, **16**(1), 800–806.

11 M. C. Brennan, S. Draguta, P. V. Kamat and M. Kuno, Light-induced anion phase segregation in mixed halide perovskites, *ACS Energy Lett.*, 2017, **3**(1), 204–213.

12 M. Yang, T. Zhang, P. Schulz, Z. Li, G. Li, D. H. Kim, N. Guo, J. J. Berry, K. Zhu and Y. Zhao, Facile fabrication of large-grain $CH_3NH_3PbI_{3-x}Br_x$ films for high-efficiency solar cells *via* CH_3NH_3Br-selective Ostwald ripening, *Nat. Commun.*, 2016, **7**(1), 1–9.

13 E. Unger, L. Kegelmann, K. Suchan, D. Sörell, L. Korte and S. Albrecht, Correction: Roadmap and roadblocks for the band gap tunability of metal halide perovskites, *J. Mater. Chem. A*, 2017, **5**(30), 15983.

14 T. M. Koh, K. Fu, Y. Fang, S. Chen, T. C. Sum, N. Mathews, S. G. Mhaisalkar, P. P. Boix and T. Baikie, Formamidinium-containing metal-halide: an alternative material for near-IR absorption perovskite solar cells, *J. Phys. Chem. C*, 2014, **118**(30), 16458–16462.

15 M. M. Lee, J. Teuscher, T. Miyasaka, T. N. Murakami and H. J. Snaith, Efficient hybrid solar cells based on meso-superstructured organometal halide perovskites, *Science*, 2012, **338**(6107), 643–647.

16 Z. Li, M. J. Yang, J. S. Park, S. H. Wei, J. J. Berry and K. Zhu, Stabilizing Perovskite Structures by Tuning Tolerance Factor: Formation of Formamidinium and Cesium Lead Iodide Solid-State Alloys, *Chem. Mater.*, 2016, **28**(1), 284–292.

17 L. Gil-Escrig, A. Miquel-Sempere, M. Sessolo and H. J. Bolink, Mixed iodide–bromide methylammonium lead perovskite-based diodes for light emission and photovoltaics, *J. Phys. Chem. Lett.*, 2015, **6**(18), 3743–3748.

18 G. E. Eperon, S. D. Stranks, C. Menelaou, M. B. Johnston, L. M. Herz and H. J. Snaith, Formamidinium lead trihalide: a broadly tunable perovskite for efficient planar heterojunction solar cells, *Energy Environ. Sci.*, 2014, **7**(3), 982–988.

19 R. E. Beal, D. J. Slotcavage, T. Leijtens, A. R. Bowring, R. A. Belisle, W. H. Nguyen, G. F. Burkhard, E. T. Hoke and M. D. McGehee, Cesium lead halide perovskites with improved stability for tandem solar cells, *J. Phys. Chem. Lett.*, 2016, **7**(5), 746–751.

20 C. C. Stoumpos and M. G. Kanatzidis, The renaissance of halide perovskites and their evolution as emerging semiconductors, *Acc. Chem. Res.*, 2015, **48**(10), 2791–2802.

21 A. Poglitsch and D. Weber, Dynamic disorder in methylammoniumtrihalogenoplumbates(II) observed by millimeter-wave spectroscopy, *J. Chem. Phys.*, 1987, **87**(11), 6373–6378.

22 J. H. Noh, S. H. Im, J. H. Heo, T. N. Mandal and S. I. Seok, Chemical management for colorful, efficient, and stable inorganic–organic hybrid nanostructured solar cells, *Nano Lett.*, 2013, **13**(4), 1764–1769.

23 V. M. Goldschmidt, Die gesetze der krystallochemie, *Naturwissenschaften*, 1926, **14**(21), 477–485.

24 C. Ji, T. Zhu, Y. Fan, Z. Li, X. Liu, L. Li, Z. Sun and J. Luo, Localized Lattice Expansion of $FAPbBr_3$ to Design a 3D Hybrid Perovskite for Sensitive Near-Infrared Photodetection, *Angew. Chem., Int. Ed.*, 2022, **61**(47), e202213294.

25 J. Ma, J. Su, Z. Lin, J. He, L. Zhou, T. Li, J. Zhang, S. Liu, J. Chang and Y. Hao, Double Side Interfacial Optimization for Low-Temperature Stable $CsPbI_2Br$ Perovskite Solar Cells with High Efficiency Beyond 16%. Energy & Environmental, *Materials*, 2022, **5**(2), 637–644.

26 Z. Li, M. Yang, J.-S. Park, S.-H. Wei, J. J. Berry and K. Zhu, Stabilizing perovskite structures by tuning tolerance factor:

formation of formamidinium and cesium lead iodide solid-state alloys, *Chem. Mater.*, 2016, **28**(1), 284–292.
27 Y. Bai, Z. Huang, X. Zhang, J. Lu, X. Niu, Z. He, C. Zhu, M. Xiao, Q. Song and X. Wei, Initializing film homogeneity to retard phase segregation for stable perovskite solar cells, *Science*, 2022, **378**(6621), 747–754.
28 S. Moradi, S. Kundu, M. Rezazadeh, V. Yeddu, O. Voznyy and M. I. Saidaminov, High-throughput exploration of halide perovskite compositionally-graded films and degradation mechanisms, *Commun. Mater.*, 2022, **3**(1), 1–5.
29 Y. Zhou, I. Poli, D. Meggiolaro, F. De Angelis and A. Petrozza, Defect activity in metal halide perovskites with wide and narrow bandgap, *Nat. Rev. Mater.*, 2021, **6**(11), 986–1002.
30 J. Even, L. Pedesseau and C. Katan, Analysis of multivalley and multibandgap absorption and enhancement of free carriers related to exciton screening in hybrid perovskites, *J. Phys. Chem. C*, 2014, **118**(22), 11566–11572.
31 C. Yi, J. Luo, S. Meloni, A. Boziki, N. Ashari-Astani, C. Grätzel, S. M. Zakeeruddin, U. Röthlisberger and M. Grätzel, Entropic stabilization of mixed A-cation ABX 3 metal halide perovskites for high performance perovskite solar cells, *Energy Environ. Sci.*, 2016, **9**(2), 656–662.
32 J. Barrier, R. E. Beal, A. Gold-Parker, J. A. Vigil, E. Wolf, L. Waquier, N. J. Weadock, Z. Zhang, L. T. Schelhas and A. F. Nogueira, Compositional heterogeneity in $Cs_yFA_{1-y}Pb(Br_xI_{1-x})_3$ perovskite films and its impact on phase behavior, *Energy Environ. Sci.*, 2021, **14**(12), 6394–6405.
33 A. Amat, E. Mosconi, E. Ronca, C. Quarti, P. Umari, M. K. Nazeeruddin, M. Gratzel and F. De Angelis, Cation-induced band-gap tuning in organohalide perovskites: interplay of spin–orbit coupling and octahedra tilting, *Nano Lett.*, 2014, **14**(6), 3608–3616.
34 N. J. Jeon, J. H. Noh, W. S. Yang, Y. C. Kim, S. Ryu, J. Seo and S. I. Seok, Compositional engineering of perovskite materials for high-performance solar cells, *Nature*, 2015, **517**(7535), 476–480.
35 S. Ašmontas, A. Čerškus, J. Gradauskas, A. Grigucevičienė, R. Juškėnas, K. Leinartas, A. Lučun, K. Petrauskas, A. Selskis and A. Sužiedėlis, Impact of Cesium Concentration on Optoelectronic Properties of Metal Halide Perovskites, *Materials*, 2022, **15**(5), 1936.
36 J. Liang, C. Chen, X. Hu, M. Xiao, C. Wang, F. Yao, J. Li, H. Wang, J. He and B. Da, Revealing the Mechanism of π Aromatic Molecule as an Effective Passivator and Stabilizer in Highly Efficient Wide-Bandgap Perovskite Solar Cells, *Sol. RRL*, 2021, **5**(8), 2100249.
37 Y. Yu, R. Liu, F. Zhang, C. Liu, Q. Wu, M. Zhang and H. Yu, Potassium tetrafluoroborate-induced defect tolerance enables efficient wide-bandgap perovskite solar cells, *J. Colloid Interface Sci.*, 2022, **605**, 710–717.
38 M. Jaysankar, W. Qiu, J. Bastos, J. Tait, M. Debucquoy, U. W. Paetzold, D. Cheyns and J. Poortmans, Crystallisation dynamics in wide-bandgap perovskite films, *J. Mater. Chem. A*, 2016, **4**(27), 10524–10531.
39 G. Longo, L. Gil-Escrig, M. J. Degen, M. Sessolo and H. J. Bolink, Perovskite solar cells prepared by flash evaporation, *Chem. Commun.*, 2015, **51**(34), 7376–7378.
40 A. Rizzo, A. Listorti and S. Colella, Chemical insights into perovskite ink stability, *Chem*, 2021, **8**(1), 31–45.
41 N. J. Jeon, J. H. Noh, Y. C. Kim, W. S. Yang, S. Ryu and S. I. Seok, Solvent engineering for high-performance inorganic–organic hybrid perovskite solar cells, *Nat. Mater.*, 2014, **13**(9), 897–903.
42 S. Ruan, M.-A. Surmiak, Y. Ruan, D. P. McMeekin, H. Ebendorff-Heidepriem, Y.-B. Cheng, J. Lu and C. R. McNeill, Light induced degradation in mixed-halide perovskites, *J. Mater. Chem. C*, 2019, **7**(30), 9326–9334.
43 C. C. Boyd, R. Cheacharoen, T. Leijtens and M. D. McGehee, Understanding degradation mechanisms and improving stability of perovskite photovoltaics, *Chem. Rev.*, 2018, **119**(5), 3418–3451.
44 Y. Li, H. Xie, E. L. Lim, A. Hagfeldt and D. Bi, Recent progress of critical interface engineering for highly efficient and stable perovskite solar cells, *Adv. Energy Mater.*, 2022, **12**(5), 2102730.
45 T. Leijtens, K. A. Bush, R. Prasanna and M. D. McGehee, Opportunities and challenges for tandem solar cells using metal halide perovskite semiconductors, *Nat. Energy*, 2018, **3**(10), 828–838.
46 J. Troughton, K. Hooper and T. M. Watson, Humidity resistant fabrication of $CH_3NH_3PbI_3$ perovskite solar cells and modules, *Nano Energy*, 2017, **39**, 60–68.
47 G. Divitini, S. Cacovich, F. Matteocci, L. Cinà, A. Di Carlo and C. Ducati, In situ observation of heat-induced degradation of perovskite solar cells. Nature, *Energy*, 2016, **1**(2), 1–6.
48 S. G. Ji, I. J. Park, H. Chang, J. H. Park, G. P. Hong, B. K. Choi, J. H. Jang, Y. J. Choi, H. W. Lim and Y. J. Ahn, Stable pure-iodide wide-band-gap perovskites for efficient Si tandem cells *via* kinetically controlled phase evolution, *Joule*, 2022, **6**(10), 2390–2405.
49 B. Suarez, V. Gonzalez-Pedro, T. S. Ripolles, R. S. Sanchez, L. Otero and I. Mora-Sero, Recombination study of combined halides (Cl, Br, I) perovskite solar cells, *J. Phys. Chem. Lett.*, 2014, **5**(10), 1628–1635.
50 S. A. Kulkarni, T. Baikie, P. P. Boix, N. Yantara, N. Mathews and S. Mhaisalkar, Band-gap tuning of lead halide perovskites using a sequential deposition process, *J. Mater. Chem. A*, 2014, **2**(24), 9221–9225.
51 E. T. Hoke, D. J. Slotcavage, E. R. Dohner, A. R. Bowring, H. I. Karunadasa and M. D. McGehee, Reversible photo-induced trap formation in mixed-halide hybrid perovskites for photovoltaics, *Chem. Sci.*, 2015, **6**(1), 613–617.
52 D. P. McMeekin, G. Sadoughi, W. Rehman, G. E. Eperon, M. Saliba, M. T. Hörantner, A. Haghighirad, N. Sakai, L. Korte and B. Rech, A mixed-cation lead mixed-halide perovskite absorber for tandem solar cells, *Science*, 2016, **351**(6269), 151–155.
53 X. Liu, Z. Wu, X. Fu, L. Tang, J. Li, J. Gong and X. Xiao, Highly efficient wide-band-gap perovskite solar cells fabricated by sequential deposition method, *Nano Energy*, 2021, **86**, 106114.
54 J. Liang, C. Chen, X. Hu, Z. Chen, X. Zheng, J. Li, H. Wang, F. Ye, M. Xiao and Z. Lu, Suppressing the phase

segregation with potassium for highly efficient and photostable inverted wide-band gap halide perovskite solar cells, *ACS Appl. Mater. Interfaces*, 2020, **12**(43), 48458–48466.

55 J. Tao, X. Liu, J. Shen, S. Han, L. Guan, G. Fu, D.-B. Kuang and S. Yang, F-Type Pseudo-Halide Anions for High-Efficiency and Stable Wide-Band-Gap Inverted Perovskite Solar Cells with Fill Factor Exceeding 84%, *ACS Nano*, 2022, **16**(7), 10798–10810.

56 D. Forgács, D. Pérez-del-Rey, J. Ávila, C. Momblona, L. Gil-Escrig, B. Dänekamp, M. Sessolo and H. J. Bolink, Efficient wide band gap double cation–double halide perovskite solar cells, *J. Mater. Chem. A*, 2017, **5**(7), 3203–3207.

57 D. H. Kim, C. P. Muzzillo, J. Tong, A. F. Palmstrom, B. W. Larson, C. Choi, S. P. Harvey, S. Glynn, J. B. Whitaker and F. Zhang, Bimolecular additives improve wide-band-gap perovskites for efficient tandem solar cells with CIGS, *Joule*, 2019, **3**(7), 1734–1745.

58 L. Gil-Escrig, C. Dreessen, F. Palazon, Z. Hawash, E. Moons, S. Albrecht, M. Sessolo and H. J. Bolink, Efficient wide-bandgap mixed-cation and mixed-halide perovskite solar cells by vacuum deposition, *ACS Energy Lett.*, 2021, **6**(2), 827–836.

59 X. Ma, J. Pan, Y. Wang, X. Gao, M. Hu, Z. Ku, Y. Ma, F. Huang, Y.-B. Cheng and J. Lu, Bromide complimented methylammonium-free wide bandgap perovskite solar modules with high efficiency and stability, *Chem. Eng. J.*, 2022, **445**, 136626.

60 U. D. Menda, G. Ribeiro, D. Nunes, T. Calmeiro, H. Águas, E. Fortunato, R. Martins and M. J. Mendes, High-performance wide bandgap perovskite solar cells fabricated in ambient high-humidity conditions, *Mater. Adv.*, 2021, **2**(19), 6344–6355.

61 N. Yan, Y. Gao, J. Yang, Z. Fang, J. Feng, X. Wu, T. Chen and S. Liu, Wide-Bandgap Perovskite Solar Cell Using a Fluoride-Assisted Surface Gradient Passivation Strategy, *Angew. Chem., Int. Ed.*, 2023, **62**(11), e202216668.

62 M. A. Mahmud, J. Zheng, S. Tang, G. Wang, J. Bing, A. D. Bui, J. Qu, L. Yang, C. Liao and H. Chen, Cation-Diffusion-Based Simultaneous Bulk and Surface Passivations for High Bandgap Inverted Perovskite Solar Cell Producing Record Fill Factor and Efficiency, *Adv. Energy Mater.*, 2022, **12**(36), 2201672.

63 A. Buin, P. Pietsch, J. Xu, O. Voznyy, A. H. Ip, R. Comin and E. H. Sargent, Materials processing routes to trap-free halide perovskites, *Nano Lett.*, 2014, **14**(11), 6281–6286.

64 C. G. Bischak, C. L. Hetherington, H. Wu, S. Aloni, D. F. Ogletree, D. T. Limmer and N. S. Ginsberg, Origin of reversible photoinduced phase separation in hybrid perovskites, *Nano Lett.*, 2017, **17**(2), 1028–1033.

65 S. Draguta, O. Sharia, S. J. Yoon, M. C. Brennan, Y. V. Morozov, J. S. Manser, P. V. Kamat, W. F. Schneider and M. Kuno, Rationalizing the light-induced phase separation of mixed halide organic–inorganic perovskites, *Nat. Commun.*, 2017, **8**(1), 1–8.

66 H. Zhang, X. Fu, Y. Tang, H. Wang, C. Zhang, W. W. Yu, X. Wang, Y. Zhang and M. Xiao, Phase segregation due to ion migration in all-inorganic mixed-halide perovskite nanocrystals, *Nat. Commun.*, 2019, **10**(1), 1–8.

67 T. Wei, K. Lian, J. Tao, H. Zhang, D. Xu, J. Han, C. Fan, Z. Zhang, W. Bi and C. Sun, Mn-Doped Multiple Quantum Well Perovskites for Efficient Large-Area Luminescent Solar Concentrators, *ACS Appl. Mater. Interfaces*, 2022, **14**(39), 44572–44580.

68 N. Ahn, K. Kwak, M. S. Jang, H. Yoon, B. Y. Lee, J.-K. Lee, P. V. Pikhitsa, J. Byun and M. Choi, Trapped charge-driven degradation of perovskite solar cells, *Nat. Commun.*, 2016, **7**(1), 1–9.

69 F. Hu, C. Yin, H. Zhang, C. Sun, W. W. Yu, C. Zhang, X. Wang, Y. Zhang and M. Xiao, Slow Auger recombination of charged excitons in nonblinking perovskite nanocrystals without spectral diffusion, *Nano Lett.*, 2016, **16**(10), 6425–6430.

70 W. Mao, C. R. Hall, S. Bernardi, Y.-B. Cheng, A. Widmer-Cooper, T. A. Smith and U. Bach, Light-induced reversal of ion segregation in mixed-halide perovskites, *Nat. Mater.*, 2021, **20**(1), 55–61.

71 S. J. Yoon, M. Kuno and P. V. Kamat, Shift happens. How halide ion defects influence photoinduced segregation in mixed halide perovskites, *ACS Energy Lett.*, 2017, **2**(7), 1507–1514.

72 M. Hu, C. Bi, Y. Yuan, Y. Bai and J. Huang, Stabilized wide bandgap $MAPbBr_xI_{3-x}$ perovskite by enhanced grain size and improved crystallinity. Advanced, *Science*, 2016, **3**(6), 1500301.

73 M. K. Kuznetsov, N. A. Emelianov, D. V. Korchagin, G. V. Shilov, S. M. Aldoshin, P. A. Troshin and L. A. Frolova, Enhanced photostability of $CsPbI_2Br$-based perovskite solar cells through suppression of phase segregation using a zwitterionic additive, *Sustainable Energy Fuels*, 2022, **6**(15), 3536–3541.

74 I. L. Braly, R. J. Stoddard, A. Rajagopal, A. R. Uhl, J. K. Katahara, A. K.-Y. Jen and H. W. Hillhouse, Current-induced phase segregation in mixed halide hybrid perovskites and its impact on two-terminal tandem solar cell design, *ACS Energy Lett.*, 2017, **2**(8), 1841–1847.

75 G. F. Samu, C. Janáky and P. V. Kamat, A victim of halide ion segregation. How light soaking affects solar cell performance of mixed halide lead perovskites, *ACS Energy Lett.*, 2017, **2**(8), 1860–1861.

76 W. Li, M. U. Rothmann, A. Liu, Z. Wang, Y. Zhang, A. R. Pascoe, J. Lu, L. Jiang, Y. Chen and F. Huang, Phase segregation enhanced ion movement in efficient inorganic $CsPbIBr_2$ solar cells, *Adv. Energy Mater.*, 2017, **7**(20), 1700946.

77 J. Hu, R. Gottesman, L. Gouda, A. Kama, M. Priel, S. Tirosh, J. Bisquert and A. Zaban, Photovoltage behavior in perovskite solar cells under light-soaking showing photoinduced interfacial changes, *ACS Energy Lett.*, 2017, **2**(5), 950–956.

78 Z. Li, X. Zheng, X. Xiao, Y. An, Y. Wang, Q. Huang, X. Li, R. Cheacharoen, Q. An and Y. Rong, Beyond the Phase Segregation: Probing the Irreversible Phase Reconstruction of Mixed-Halide Perovskites, *Adv. Sci.*, 2022, **9**(5), 2103948.

79 N. H. Nickel, F. Lang, V. V. Brus, O. Shargaieva and J. Rappich, Unraveling the light-induced degradation mechanisms of $CH_3NH_3PbI_3$ perovskite films, *Adv. Electron. Mater.*, 2017, **3**(12), 1700158.
80 J. Yang, X. Liu, Y. Zhang, X. Zheng, X. He, H. Wang, F. Yue, S. Braun, J. Chen and J. Xu, Comprehensive understanding of heat-induced degradation of triple-cation mixed halide perovskite for a robust solar cell, *Nano Energy*, 2018, **54**, 218–226.
81 V. V. Travkin, P. A. Yunin, A. N. Fedoseev, A. I. Okhapkin, Y. I. Sachkov and G. L. Pakhomov, Wavelength-selective degradation of perovskite-based solar cells, *Solid State Sci.*, 2020, **99**, 106051.
82 T. Leijtens, G. E. Eperon, S. Pathak, A. Abate, M. M. Lee and H. J. Snaith, Overcoming ultraviolet light instability of sensitized TiO_2 with meso-superstructured organometal tri-halide perovskite solar cells, *Nat. Commun.*, 2013, **4**(1), 1–8.
83 D. Wei, T. Wang, J. Ji, M. Li, P. Cui, Y. Li, G. Li, J. M. Mbengue and D. Song, Photo-induced degradation of lead halide perovskite solar cells caused by the hole transport layer/metal electrode interface, *J. Mater. Chem. A*, 2016, **4**(5), 1991–1998.
84 A. Farooq, M. R. Khan, T. Abzieher, A. Voigt, D. C. Lupascu, U. Lemmer, B. S. Richards and U. W. Paetzold, Photodegradation of triple-cation perovskite solar cells: the role of spectrum and bias conditions, *ACS Appl. Energy Mater.*, 2021, **4**(4), 3083–3092.
85 R. Zhao, Z. Gu, P. Li, Y. Zhang and Y. Song, Flexible and Wearable Optoelectronic Devices Based on Perovskites, *Adv. Mater. Technol.*, 2022, **7**(3), 2101124.
86 L. Duan and A. Uddin, Defects and Stability of Perovskite Solar Cell: A Critical Analysis, *Mater. Chem. Front.*, 2022, **6**(4), 400–417.
87 W. Tress, Perovskite solar cells on the way to their radiative efficiency limit-insights into a success story of high open-circuit voltage and low recombination, *Adv. Energy Mater.*, 2017, **7**(14), 1602358.
88 X. Wei, M. Xiao, B. Wang, C. Wang, Y. Li, J. Dou, Z. Cui, J. Dou, H. Wang and S. Ma, Avoiding structural collapse to reduce lead leakage in perovskite photovoltaics, *Angew. Chem.*, 2022, **134**(27), e202204314.
89 Z. Wang, Q. Lin, F. P. Chmiel, N. Sakai, L. M. Herz and H. J. Snaith, Efficient ambient-air-stable solar cells with 2D–3D heterostructured butylammonium-caesium-formamidinium lead halide perovskites, *Nat. Energy*, 2017, **2**(9), 1–10.
90 B. Philippe, B.-W. Park, R. Lindblad, J. Oscarsson, S. Ahmadi, E. M. Johansson and H. Rensmo, Chemical and Electronic Structure Characterization of Lead Halide Perovskites and Stability Behavior under Different Exposures A Photoelectron Spectroscopy Investigation, *Chem. Mater.*, 2015, **27**(5), 1720–1731.
91 B. Chen, N. Ren, Y. Li, L. Yan, S. Mazumdar, Y. Zhao and X. Zhang, Insights into the development of monolithic perovskite/silicon tandem solar cells, *Adv. Energy Mater.*, 2022, **12**(4), 2003628.
92 J. Wu, S.-C. Liu, Z. Li, S. Wang, D.-J. Xue, Y. Lin and J.-S. Hu, Strain in perovskite solar cells: origins, impacts and regulation, *Natl. Sci. Rev.*, 2021, **8**(8), nwab047.
93 J. Cao, S. X. Tao, P. A. Bobbert, C. P. Wong and N. Zhao, Interstitial occupancy by extrinsic alkali cations in perovskites and its impact on ion migration, *Adv. Mater.*, 2018, **30**(26), 1707350.
94 H. Shen, J. Peng, D. Jacobs, N. Wu, J. Gong, Y. Wu, S. K. Karuturi, X. Fu, K. Weber and X. Xiao, Mechanically-stacked perovskite/CIGS tandem solar cells with efficiency of 23.9% and reduced oxygen sensitivity, *Energy Environ. Sci.*, 2018, **11**(2), 394–406.
95 M. Abdi-Jalebi, Z. Andaji-Garmaroudi, S. Cacovich, C. Stavrakas, B. Philippe, J. M. Richter, M. Alsari, E. P. Booker, E. M. Hutter and A. J. Pearson, Maximizing and stabilizing luminescence from halide perovskites with potassium passivation, *Nature*, 2018, **555**(7697), 497–501.
96 A. Rajagopal, R. J. Stoddard, S. B. Jo, H. W. Hillhouse and A. K.-Y. Jen, Overcoming the photovoltage plateau in large bandgap perovskite photovoltaics, *Nano Lett.*, 2018, **18**(6), 3985–3993.
97 R. J. Stoddard, A. Rajagopal, R. L. Palmer, I. L. Braly, A. K.-Y. Jen and H. W. Hillhouse, Enhancing defect tolerance and phase stability of high-bandgap perovskites *via* guanidinium alloying, *ACS Energy Lett.*, 2018, **3**(6), 1261–1268.
98 A. F. Palmstrom, G. E. Eperon, T. Leijtens, R. Prasanna, S. N. Habisreutinger, W. Nemeth, E. A. Gaulding, S. P. Dunfield, M. Reese and S. Nanayakkara, Enabling flexible all-perovskite tandem solar cells, *Joule*, 2019, **3**(9), 2193–2204.
99 J. Xu, C. C. Boyd, Z. J. Yu, A. F. Palmstrom, D. J. Witter, B. W. Larson, R. M. France, J. Werner, S. P. Harvey and E. J. Wolf, Triple-halide wide-band gap perovskites with suppressed phase segregation for efficient tandems, *Science*, 2020, **367**(6482), 1097–1104.
100 J. Cho and P. V. Kamat, How chloride suppresses photo-induced phase segregation in mixed halide perovskites, *Chem. Mater.*, 2020, **32**(14), 6206–6212.
101 J. Cho and P. V. Kamat, Photoinduced phase segregation in mixed halide perovskites: thermodynamic and kinetic aspects of Cl–Br segregation, *Adv. Opt. Mater.*, 2021, **9**(18), 2001440.
102 M. B. Faheem, B. Khan, C. Feng, M. U. Farooq, F. Raziq, Y. Xiao and Y. Li, All-inorganic perovskite solar cells: energetics, key challenges, and strategies toward commercialization, *ACS Energy Lett.*, 2019, **5**(1), 290–320.
103 Y. Yang and J. You, Make perovskite solar cells stable, *Nature*, 2017, **544**(7649), 155–156.
104 M. H. Li, J. Y. Shao, Y. Jiang, F. Z. Qiu, S. Wang, J. Zhang, G. Han, J. Tang, F. Wang and Z. Wei, Electrical Loss Management by Molecularly Manipulating Dopant-free Poly(3-hexylthiophene) towards 16.93% $CsPbI_2Br$ Solar Cells, *Angew. Chem., Int. Ed.*, 2021, **133**(30), 16524–16529.
105 Y. Deng, X. Zheng, Y. Bai, Q. Wang, J. Zhao and J. Huang, Surfactant-controlled ink drying enables high-speed deposition of perovskite films for efficient photovoltaic modules, *Nat. Energy*, 2018, **3**(7), 560–566.

106 W. Qian, X. Xu, J. Wang, Y. Xu, J. Chen, Y. Ge, J. Chen, S. Xiao and S. Yang, An aerosol-liquid-solid process for the general synthesis of halide perovskite thick films for direct-conversion X-ray detectors, *Matter*, 2021, **4**(3), 942–954.

107 S. Braunger, L. E. Mundt, C. M. Wolff, M. Mews, C. Rehermann, M. Jošt, A. Tejada, D. Eisenhauer, C. Becker and J. A. Guerra, Cs_xFA_{1-x} Pb $(I_{1-y}Br_y)_3$ Perovskite Compositions: the Appearance of Wrinkled Morphology and its Impact on Solar Cell Performance, *J. Phys. Chem. C*, 2018, **122**(30), 17123–17135.

108 K. A. Bush, N. Rolston, A. Gold-Parker, S. Manzoor, J. Hausele, Z. J. Yu, J. A. Raiford, R. Cheacharoen, Z. C. Holman and M. F. Toney, Controlling thin-film stress and wrinkling during perovskite film formation, *ACS Energy Lett.*, 2018, **3**(6), 1225–1232.

109 Q. Jiang, J. Tong, R. A. Scheidt, X. Wang, A. E. Louks, Y. Xian, R. Tirawat, A. F. Palmstrom, M. P. Hautzinger and S. P. Harvey, Compositional texture engineering for highly stable wide-bandgap perovskite solar cells, *Science*, 2022, **378**(6626), 1295–1300.

110 Z. Zeng, J. Zhang, X. Gan, H. Sun, M. Shang, D. Hou, C. Lu, R. Chen, Y. Zhu and L. Han, In situ grain boundary functionalization for stable and efficient inorganic $CsPbI_2Br$ perovskite solar cells, *Adv. Energy Mater.*, 2018, **8**(25), 1801050.

111 F.-Z. Qiu, M.-H. Li, S. Wang, J.-Y. Sun, Y. Jiang, J.-J. Qi and J.-S. Hu, Regulating the crystalline phase of intermediate films enables $FA_{1-x}MA_xPbI_3$ perovskite solar cells with efficiency over 22%, *J. Mater. Chem. A*, 2021, **9**(42), 24064–24070.

112 T. Y. Yang, G. Gregori, N. Pellet, M. Grätzel and J. Maier, The significance of ion conduction in a hybrid organic–inorganic lead-iodide-based perovskite photosensitizer, *Angew. Chem., Int. Ed.*, 2015, **127**(27), 8016–8021.

113 D. Kim, H. J. Jung, I. J. Park, B. W. Larson, S. P. Dunfield, C. Xiao, J. Kim, J. Tong, P. Boonmongkolras and S. G. Ji, Efficient, stable silicon tandem cells enabled by anion-engineered wide-bandgap perovskites, *Science*, 2020, **368**(6487), 155–160.

114 J. Kim, M. I. Saidaminov, H. Tan, Y. Zhao, Y. Kim, J. Choi, J. W. Jo, J. Fan, R. Quintero-Bermudez and Z. Yang, Amide-catalyzed phase-selective crystallization reduces defect density in wide-bandgap perovskites, *Adv. Mater.*, 2018, **30**(13), 1706275.

115 Y. Zhou, Y. H. Jia, H. H. Fang, M. A. Loi, F. Y. Xie, L. Gong, M. C. Qin, X. H. Lu, C. P. Wong and N. Zhao, Composition-tuned wide bandgap perovskites: From grain engineering to stability and performance improvement, *Adv. Funct. Mater.*, 2018, **28**(35), 1803130.